Special Section on Computational Fabrication

KinetiX - designing auxetic-inspired deformable material structures

Jifei Ou [a,*], Zhao Ma [b,1], Jannik Peters [c,1], Sen Dai [a], Nikolaos Vlavianos [a], Hiroshi Ishii [a]

[a] *Massachusetts Institute of Technology, United States*
[b] *ETH, Zürich, Switzerland*
[c] *RWTH, Aachen, Germany*

ARTICLE INFO

ABSTRACT

This paper describes a group of auxetic-inspired material structures that can transform into various shapes upon compression. We developed four cellular-based material structure units composed of rigid plates and elastic/rotary hinges. Different compositions of these units lead to a variety of tunable shape-changing possibilities, such as uniform scaling, shearing, bending and rotating. By tessellating those transformations together, we can create various higher level transformations for product design. In the paper, we first give a geometrical and numerical description of the units' configuration and their degrees of freedom. An interactive simulation tool is developed for users to input designed structures and preview the transformation. Finally we present three application prototypes that utilize our proposed structures.

Published by Elsevier Ltd.

1. Introduction

Materials are a fundamental part of how we interact with the world. Recent advances in fabrication technology have enabled a new field of tunable materials with tailored properties. Recently, within the domains of Human-Computer Interaction (HCI) and Computer Graphics (CG), there has been a growing interest in designing tunable material systems that allow deformable physical shapes/structures [1–3]. In addition, novel transformation mechanisms [4–7] and applying responsive materials [8–10] open up a wide design space for researchers to prototype shape-changing materials for design. These works investigate how to integrate energy sources (heat, air pressure, humidity, etc.) and transformation mechanisms into an interactive system.

In this paper, we propose a deformable material mechanism called KinetiX. We extend an auxetic mechanism to a set of novel cell configurations that enables multiple deformations. An auxetic material [11] is a material that exhibits a Negative Poisson's Ratio (NPR). Unlike conventional materials, when an auxetic material is stretched (or compressed) in one direction, instead of becoming thinner (or thicker), it becomes thicker (or thinner) in perpendicular directions. While the majority of the studies of auxetic materials focus on their mechanical properties and topological variations [12], our work proposes a parametric design approach that gives auxetic structures the ability to deform beyond shrinking or

expanding. To do so, we see the auxetic structure as a parametric four-bar linkage. By reconfiguring the location and angle of the hinges, each unit acquires a unique transformation, such as uniform scaling, shearing, folding and twisting. We also find the transformation of those configurations to be parametrically tunable. To further assist the design using KinetiX structures, we developed a physics-based simulation environment to interactively deform and preview a given design. In addition, we demonstrate several integrations of two or more unit configurations in one structure to create larger deformable shapes.

In contrast to previous work [6], our system enables transformations beyond 2D shearing. The mechanism exhibits a controlled single degree of freedom (DoF), and therefore can achieve global transformations with local deformation. These mechanisms are also highly modular, enabling the ability to scale.

Our contributions are

- Describing the parameters of an auxetic-inspired structure to achieve planar and spatial transformations;
- A simulation environment that predicts the deformations before fabrication;
- Three application prototypes to show KinetiX structure integrated in product design.

The main goal of this research is to demonstrate a set of cell configurations for mechanical deformation design. As auxetic materials gain increasing interests in computational fabrication, our work provides novel cell designs for further studies on deformable materials. We also hope our contribution will be useful for future HCI researchers to integrate such mechanisms with sensors and actuators for future interactive systems.

* Corresponding author.
  E-mail address: ishii@media.mit.edu (H. Ishii).
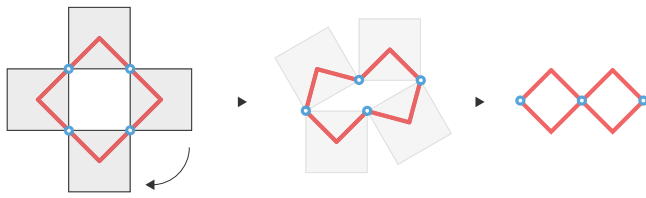[1] The work was conducted when the author studied at MIT.

Fig. 1. Rotating polygon type auxetic material simplified as a four-bar linkage structure.

2. Related works

2.1. Metamaterials and auxetic materials

Auxetics is a group of mechanical metamaterials that exhibits an NPR. Unlike conventional materials, when a piece of auxetic material is stretched (or compressed) in one direction, instead of becoming thinner (or thicker), it becomes thicker (or thinner) in perpendicular directions. Since the discovery of the first auxetic material, many studies have shown numerous structural designs of materials that exhibit the auxeticity [13,14]. Studies have also demonstrated that, beyond possessing an NPR, auxetic materials exhibit other enhanced mechanical properties such as shear resistance[15], indentation resistance[16] and fracture toughness[17]. It also demonstrates enhanced sound and vibration absorption properties[18]. Based on these properties, researchers have been exploring applications of auxetic structures for smart valves and filters; tunable phononic and photonic materials [19]; etc. Inspired by these prior works in auxetic structures, our work proposes design parameters that give auxetic structures the ability to deform beyond planar shrinking. These new cell configurations also allow the material to spatially twist and bend parametrically.

2.2. Linkage-based transformation design

Design of linkage-based structures has a long history in mechanical engineering. Previous work [20] shows a linkage structure can be used to design transformable toys and buildings. Many of configurations similar to this have been widely presented in the design practice [21]. Recent work presented a mathematical framework of a known origami structure, which was used to design a transformable material [22]. Inspired by this work, we present a linkage-based structure that has a set of different deformations and is limited to one DoF.

2.3. Programmable materials in CG and HCI

Recent research in CG and HCI has been investigating how to digitally manipulate material composition and structures to create predictable shape-changes or property changes [23–25]. This includes both how to adapt responsive materials in an interactive system [8], and material composition strategies to create programmable material transformations [5,6]. While most of the studies focus on layer by layer composites to create desirable transformations, this work shows that by assembling a hinge structure into four configurations, we could achieve various linear and surface shape-changes.

3. Unit cell transformation

Among many types of auxetic material structures, the Rotating Polygon [12,14,26] is one of the most popular subjects to study. It contains four rectangles that are connected by their vertices. This configuration can be simplified as a four-bar linkage structure as shown in Fig. 1. This is where our work started. In this section, we
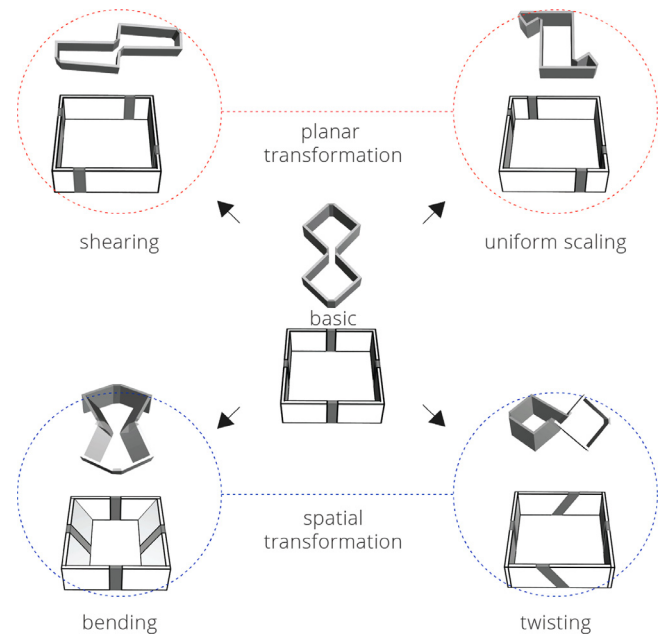

Fig. 2. The design parameters of KinetiX. From the basic unit, a planar and spatial transformation can be created. Parametrically shifting the position of the hinge creates uniform scaling and shearing; rotating the hinge in or out-of-plane creates twisting and bending.

describe how our designed mechanism originated from this planar four-bar linkage, and also show an extended version that enables planar and spatial transformations. In general, we can give five parameters to a hinge on one bar: translations in three axis and rotations in two axis. This work focuses on the translation on the bar and the two rotations(see below) to keep the rectangular shape of a unit. In all four configurations we present here, the hinge parameters are operated in a symmetrical manner. That is, the parameters of the hinge on one bar, are duplicated or mirrored to the other bars. While arbitrarily assigning values to those parameters could also create a transformable unit cell, our experiments are built on the simplified situation.

3.1. Basic

The basic mechanism of KinetiX material is based on a four-bar linkage connected by four rotary joints (hinges). By parametrically placing four hinges on the four sides of a rigid square unit respectively, we are able to transform the rigid unit in designated ways, both planar and spatially (Fig. 2). We explain the geometric as well as mathematical details below.

3.2. Planar transformation

The planar transformation is derived directly from the planar quadrilateral linkage. By limiting the four side-plates in the vertical direction, and all hinges to be only horizontally rotatable, the unit can only be transformed in the 2D space. We thus define a square frame c_i $(i = 0, 1, 2, 3)$ and arbitrarily place four hinges h_i $(i = 1, 2, 3, 4)$ on the four sides (Fig. 3) and construct a linkage system by connecting the four hinges sequentially. Since each triangle, composed by every bar and the neighbouring "L" shape partial frame divided by two hinges, i.e. $\triangle h_0 c_1 h_1$, $\triangle h_1 c_2 h_2$, $\triangle h_2 c_3 h_3$, $\triangle h_3 c_0 h_0$, has zero DoF, the transformation of the frame through the rotations of the hinges are fully defined by the transformation of linkage l_0, l_1, l_2, l_3.

Chebychev–Grübler–Kutzbach mobility formula is used to decide the DoF of a kinematic chain. The linkage form (a special case
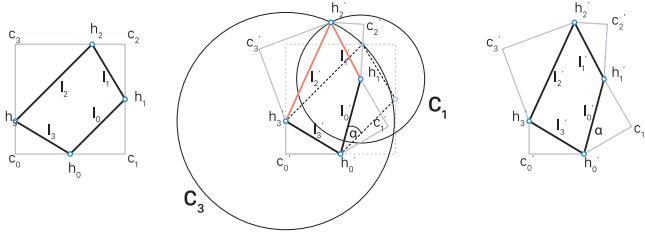
Fig. 3. Planar transformation deduced from the geometric relationship of intersecting circles.
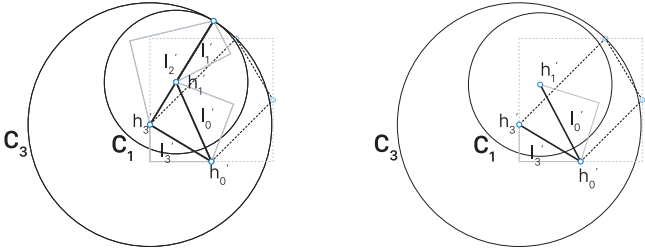

Fig. 4. Hinge locations that result tangent and disjoint states.
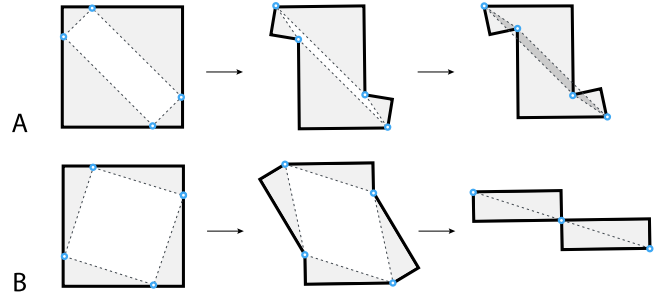

Fig. 5. A. Crossable linkage. Collision does not happen and the frame can continue to transform after the four-bar linkage coincide on a line. Hinges on the linkage will pass through the bars. $P = (0.8, 0.2, 0.8, 0.2)$; B. Uncrossable linkage. Collision occurs and the frame cannot continue to transform when the four-bar linkage coincide on a line. $P = (0.8, 0.8, 0.8, 0.8)$.
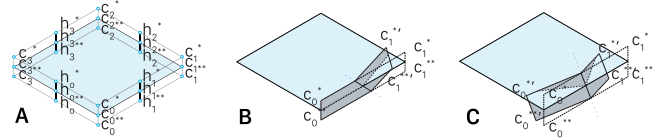

Fig. 6. (A). 3D hinged frame unit and labeling convention; (B). Hinge in-plane rotation; (C). Wall plane rotation.

of rigid body) of this formula is:

$$M = 3(N - 1 - j) + \sum_{i=1}^{j} f_i \qquad (1)$$

where N is the number of rigid bodies (bars here), j is the number of joints, and f_i is the DoF of each joint (1 for planar hinge). For the above simple four-bar linkage, it is straight-forward to find its DoF as $M = 1$.

We fix bar l_3 and provide a counter-clockwise rotation α to bar l_0, as shown in Fig. 3. The new position h'_1 of hinge h_1 is decided uniquely by the rotation and the new position h'_2 of hinge h_2 is decided uniquely by the intersection of two circles C_1 and C_3, which are centered at h'_1 and h'_3 with radii l_1 and l_2, respectively. For different rotations, the relationship between the two circles may vary from intersected to tangent or disjoint states (Fig. 4). Notice that when there are two intersection points, the one that creates a bar-intersection should be discarded.

We parameterize the locations of the hinges with a parameter $t \in [0, 1]$ on the vector $\mathbf{H} = [c_i, \ c_{i+1 \ (mod \ 4)}], \quad i = 0, 1, 2, 3$ of the frame edges and use the above configuration to examine the exact transformation of the rigid frame. For a single four-edge frame, a position combination is defined as

$$P = (t_0, \ t_1, \ t_2, \ t_3), \quad t_i \in [0, 1] \qquad (2)$$

Through a brief exploration, we found the magnitude of an executable transformation to be correlated with this combination. Fig. 5 shows how P affects the collision through two typical types:

- *Crossable linkage* Repetitive hinge position parameters for four edges, namely $P = (k, \ (1 - k), \ k, \ (1 - k))$, $k \in (0, 1)$. The hinges form a parallelogram linkage in the center of the frame structure. When transforming, the maximum transformable state happens after the linkage merged into a line and cross the corresponding bars, as shown in Fig. 5.A [6]. This configuration resembles the re-entrant cell design [26]. The magnitude of the crossable linkage transformation can be calculated by the final area of the transformed state:

$$R_a = (2 + \sqrt{2})k^2 - (2 + \sqrt{2})k + 1,$$
$$k \in [0, 0.5) \cup (0.5, 1] \qquad (3)$$

where k is the position of the hinge. As one can see, the closer the k is to 0 or 1, the less the unit cell will shrink when subject to a deformation;

- *Uncrossable linkage.* Same hinge position parameter for all four edges, namely $P = (k, \ k, \ k, \ k)$, $k \in (0, 1)$. The hinges form a square linkage in the center of the frame structure. When transforming, the maximum transformable state is reached when the linkage merged into a line, as shown in Fig. 5.B. As it transformed, the two smaller cells form a shearing angle, which can be calculated as follows:

$$\tan \theta = \frac{1 - k}{k}, k \in (0, 0.5) \cup (0.5, 1] \qquad (4)$$

where k is the position of the hinge; As one can see, the closer the k is to 0 or 1, the more the unit cell will shear when subject to a deformation.

The key constraints here for the transformation are the divided geometries of the original rigid frame.

Though numerous configurations for shifting the four hinges' position exists, the above two types of symmetrical operation create unique transformations that resemble uniform scaling and shearing and give rise to further more design ideas in the following sections:

3.3. Spatial transformation

Now, if we consider out-of-plane rotation of the hinges, the planar quadrilateral linkage will be transformed into a spatial system. Fig. 6.A defines a basic unit of the 3D rigid frame through a simple perpendicular extrusion of the original 2D rigid frame described in Section 3.2. The original frame c_0, c_1, c_2, c_3 now becomes the neutral plane and corresponding vertices c_i^* and c_i^{**} define the new vertical edges $E = (c_i^*, \ c_i^{**})$.

Except for the hinge axis itself, the hinge can be rotated in two orthogonal directions: one in the plane defined by the wall vector of the frame and the vertical direction, the other in the plane defined by the normal of the previous plane and the vertical direction. Two types of rotation are thus defined: one rotates only one part of the original wall out of the plane p_i and perpendicular to the original wall $W(c_i^*, \ c_{i+1}^*, \ c_{i+1}^{**}, \ c_i^{**})$ (Fig. 6.B), the other pushes
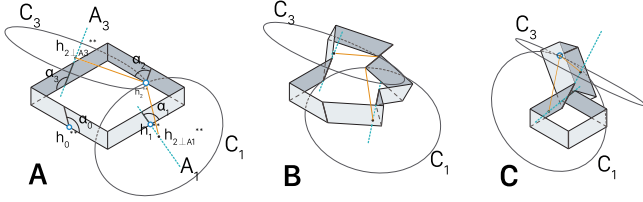
Fig. 7. (A). Initial transformation setup of hinge in-plane rotation with corresponding labelling conventions; (B). Unmatched state during the transformation; (C). special matched state with angle combination $A_{in-plane} = (\frac{\pi}{2}, \alpha, \frac{\pi}{2}, \alpha)$.

Fig. 8. (A). Initial transformation setup of out-of-plane rotation with corresponding labelling conventions; (B). Maximum transformation states under $A_{wall-rot} = (\beta_m, -\beta_n, \beta_m, -\beta_n)$; (C). Maximum transformation state under $A_{wall-rot} = (\beta_m, \beta_n, \beta_m, \beta_n)$.

both of the parts out of this neutral plane (Fig. 6.C). We will discuss these two types of 3D transformations below respectively.

3.3.1. Hinge in-plane rotation

For this case, we constrain the four-edge wall of the unit to be vertical and perpendicular to the frame plane. We conducted a similar process as the planar circumstance described in Section 3.2 for an extruded 3D frame with additional rotation angle combination (Fig. 7.A):

$$A_{in-plane} = (\alpha_0, \alpha_1, \alpha_2, \alpha_3) \quad (5)$$

where α_i describes the corresponding rotation angle of the hinge from a horizontal stage starting from the edge vector direction. A combination of $(\frac{\pi}{2}, \frac{\pi}{2}, \frac{\pi}{2}, \frac{\pi}{2})$ will result in the same structure and transformation as the planar cases.

One difference from Fig. 7.A is that the two circles constructed from the hinges with radii of corresponding linkage bar lengths will be out of the frame plane as long as the corresponding rotation angle $\alpha_i \neq \frac{\pi}{2}$, and the centers will move from h_i^{**} to the projection of the target hinge points to the rotation axis A_i, namely $h_{i\perp A_j}^{**}$. Radii also change from the length between two hinge points to the projected length (labeled orange).

Unlike the planar case, the two circles do not always intersect spatially. Though there might be a few angle combinations that guarantee an intersection of the two circles, it is almost impossible to find continuous paths that allow a smooth transformation of the frame structure (Fig. 7.B).

A special case in this category of spatial transformation is the angle combination $A_{in-plane} = (\frac{\pi}{2}, \alpha, \frac{\pi}{2}, \alpha)$ under position combination $P = (0.5, 0.5, 0.5, 0.5)$ where α is an arbitrary angle in $(0, \pi)$ and also constrained by the size of the edge wall (the hinge should be connected to the upper/lower edge of the frame). This combination creates a *"twist"* effect of the original frame by transforming the frame symmetrically, as shown in Fig. 7.C. It is simple to deduce that each of the two small cells is a planar square-like cell and that all of its inner angles are $\frac{\pi}{2}$. Considering the symmetry property of the two small cells, the "twisting" angle γ of the two planes defined by the two small square cells is given by

$$\cot \frac{\gamma}{2} = \cot \alpha \cdot \sin 45° \quad (6)$$

Unfortunately, even with this special case, only the initial state and the state in Fig. 7.C can be geometrically solved. Thus, geometric transformation cannot be established. However, this two-stage-stability constraint can be overcome to some extent with the elasticity properties of the material and the tolerance of the hinge in reality. We 3D printed several samples of size 3 by 3 cm with rotary hinges. To our surprise, the samples exhibit little resistance to the transformation, though the geometry will transform to the stable state automatically when passing the middle stage, given the hinges are sufficiently smooth. For details of the physical hinge tolerance test, please see Section 5.1.
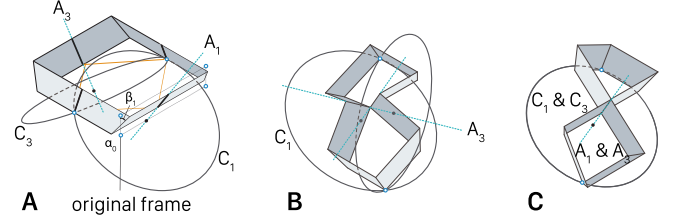
3.3.2. Hinge out-plane rotation

In the out-plane rotation, we constrain the four hinges with angle combination $(\alpha_i = \frac{\pi}{2})$ but give additional rotation β_i to each of the four edge walls around the neutral axis (Fig. 8.A). We only consider $P = (0.5, 0.5, 0.5, 0.5)$ and every pair of two facing edge walls with the same β_i here for a possible smooth transformation path, as the symmetry provides equal radii of the two circles C_1 and C_3 as well as transformation paths along each other mutually.

The out-of-plane rotation combination is defined similarly as Eq. (5):

$$A_{out-plane} = (\beta_0, \beta_1, \beta_2, \beta_3) \quad (7)$$

where $\beta_i \in (-\frac{\pi}{2}, \frac{\pi}{2})$ is the rotation of the ith corresponding edge wall. A rotation established in the same way as in Section 3.2 will transform the frame structure smoothly, as shown in Fig. 8.B and Fig. 8.C. This combination creates a *"bend"* effect of the original frame by transforming the frame symmetrically.

The difference between the two transformations is given by the two different sets of out-plane rotation combinations:

$$\begin{cases} A_{out-plane, B} = (\beta_m, -\beta_n, \beta_m, -\beta_n) \\ A_{out-plane, C} = (\beta_m, \beta_n, \beta_m, \beta_n) \end{cases} \quad (8)$$

In other words, the two pairs of walls in Fig. 8.B and Fig. 8.C are rotated inwards and outwards respectively and simultaneously. $\beta_m = \beta_n$ is not a necessary condition here. Interestingly in Fig. 8.C, the two circles and corresponding hinges coincide into one single line when the frame is transformed to the maximum state.

3.4. Unit tessellation

An intriguing question is whether we can compose a grid-like mechanism by combining multiple units of the aforementioned types and still maintain the transformable properties. This could be answered by calculating the DoF again. Given a 3×5 grid-like frame system composed with hinge position combinations:

$$P_{i,j} = \begin{cases} (0.2, 0.8, 0.2, 0.8), & \text{if } |i-j| = 0 \ (mod\ 2) \\ (0.8, 0.2, 0.8, 0.2), & \text{if } |i-j| = 1 \ (mod\ 2) \end{cases} \quad (9)$$

Through Eq. (1), we again find the DoF of the system is $M = 1$. It is relatively simple to prove that for a grid-like frame system composed with the system described here, we can always find a DoF of $M = 1$ by implementing DoF cancellation of certain joints.

The presented grid transformation of this definition is shown in Fig. 9 while Fig. 10 also shows the other typical designs with position combinations:

$$P_{i,j} = \begin{cases} (0.3, 0.3, 0.3, 0.3), & \text{if } |i-j| = 0 \ (mod\ 2) \\ (0.7, 0.7, 0.7, 0.7), & \text{if } |i-j| = 1 \ (mod\ 2) \end{cases} \quad (10)$$

The maximum transformation state where the collision of the frame structure occurs is shown in Fig. 9.D and Fig. 10.C, whereas Fig. 10.D shows an impossible state transformations. Notice that a real physical model may not be able to reach such a maximum
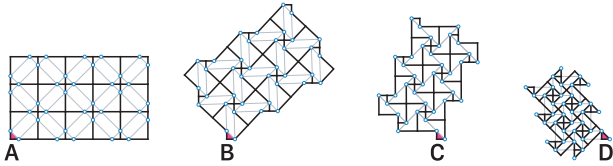
Fig. 9. Transformation of a 3×5 grid-like tessellation with crossable linkage. (A). Initial setup of the frame; B. 45° rotation; C. 90° rotation; D. 135° rotation. The initial fixed triangle at the left-bottom corner is labeled in pink.

Fig. 10. Transformation of a 3×5 grid-like tessellation with uncrossable linkage. (A). Initial setup of the frame; (B). 45° rotation; (C). 90° rotation; (D). some $> 90°$ rotation in which frame parts start to intersect and produce physical collision in reality. The initial fixed triangle at the left-bottom corner is labeled in pink.
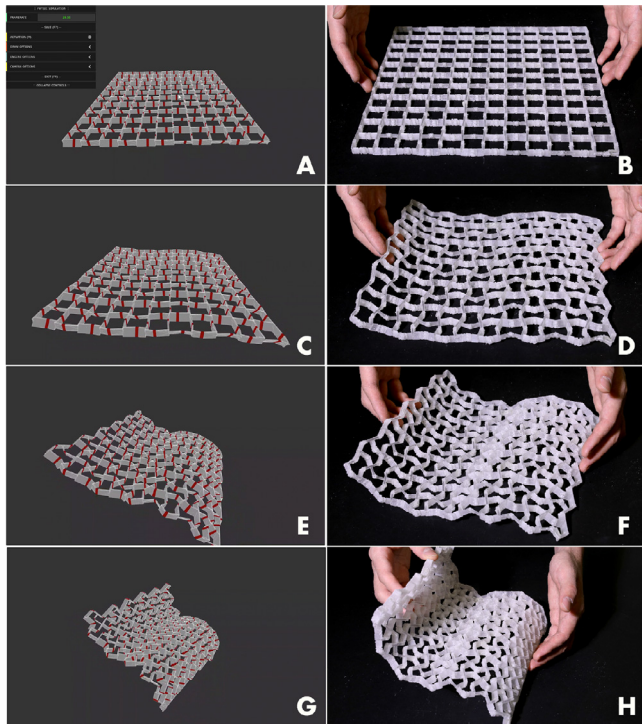
Fig. 11. The simulation environment of KinetiX. A,C,E,G show the simulation of a sheet transformation; B,D,F,H show that the fabricated material transformation matches our simulation.

stage since the thickness of the edges could potentially prevent transformations before this extreme arrangement. Special treatment in the design of the hinge and thickness are needed to overcome this difficulty. More grid-like examples are shown in Section 5.

A tessellation of both hinge in-plane and out-plane rotation unit are possible, when combined with the basic or planar transformation unit. Examples are provided in Section 5.

4. Simulation tool

As mentioned in the previous section, the twisting transformation module (hinge in-plane rotation) is possible in the physical model but not in the geometric analysis. This is due to the physi-

cal tolerance of the hinge design and the given material property. In our paper, all the hinges are either designed as a single elastic block, or a rigid rotating hinge. In either case, the material can be slightly stretched out of the rotation plane without breaking, or it can move slightly within the space inside the hinge. Therefore, instead of doing a geometric simulation, we implemented a physics-based simulation environment. For this paper, we implemented the hinge as a rotary hinge with elastic behavior.

We chose not to use a mechanically accurate but non-real-time finite element simulation library like VegaFEM or Abaqus, as we would like to have interactive control in the simulation. Furthermore, such finite element approaches quickly become very complex and computationally expensive without as much flexibility regarding contact surface determination and interaction computation. Our simulation environment is flexible and provides the option to interact with the structure by introducing additional forces. Each rigid part can be dragged or fixed individually to simulate multiple shape-change reactions. Finally, to be able to further evaluate the simulation results, the current configuration of the KinetiX structure can be exported. The software automatically prepares a complete structure file and individual files for each component type, hard and soft.

Our simulator utilizes the Bullet physics engine [27] to achieve a realistic, reliable and fast computation. The nearly rigid parts of a KinetiX structure are introduced into the simulation as perfectly rigid bodies whereas the elastic parts are transformed into active six degree of freedom constraints. Bullet physics includes the class *btGeneric6DofSpring2Constraint* which already provides the necessary methods to simulate the elastic behavior through the introduction of additional forces. However, as Bullet physics constraints are point-based, we represent each three dimensional elastic hinge by two constraint points which coincide with the main rotational axis of the elastic part. We calculate this axis based upon the initial shape of the hinge and the arrangement of the rigid parts around it. It is not only used to position the constraint points but also to calculate the reaction forces, which result from and contribute to the motion of the connected rigid parts. To achieve more realistic behavior and enforce our main rotational axis, we calculate these forces for each hinge individually with respect to its current posture in the 3D space.

Another benefit of Bullet physics is its contact algorithm implementation which is crucial for a realistic simulation of a collapsing structure like KinetiX. The deformation of KinetiX, especially at its deformation limits, highly depends on the collision of its modular parts. Accordingly, realistic and reliable contact surface determination and interaction computation is an important factor. Furthermore, a physics engine like Bullet usually allows for error terms inside the motion calculation to allow for real-time computation. Our simulator utilizes this feature to process the play inside the hinges while maintaining structural consistency. The small amount of play, which is permitted through the engine and its solver, is controlled by the hinge constraint through its error reduction parameter. The constraints in the presented implementation enforce an error reduction of 95% in each step of the simulation.

Other important packages are the Volumetric-Hierarchical Approximate Convex Decomposition (V-HACD) version 2.0 library [28] and the openFrameworks toolkit. The V-HACD library enables the representation of any designed shape that is part of a KinetiX structure through a set of approximating convex shapes. This step is crucial for acceptable computation times as the contact or intersection calculation of concave bodies would be more complex and time-consuming. Furthermore, it allows for a fast input pipeline, as the parts of the three dimensional structural design are automatically prepared and converted into appropriate representations for Bullet physics. The openFrameworks toolkit facilitates the visualization of the process and, due to its modularity and respective

add-ons, the creation of an intuitive and comprehensive graphical user interface. Furthermore, it already provides model loader functionality to read in the designs.

In summary, the final model is based on the fundamental mathematical formulations of multi-body dynamics for closed-loop kinematic chains. Open chains would enable the usage of generalized coordinates but for KinetiX the description is in absolute coordinates. This means describing all rigid bodies with six degrees of freedom each is necessary. Accordingly, each rigid component i is represented mathematically by its position vector:

$$\mathbf{r}_i^0 = \{x_i^0, y_i^0, z_i^0, \alpha_i^0, \beta_i^0, \gamma_i^0\} \tag{11}$$

in the global space and each soft part j is entered into the system as a set of time-independent constraint equations which limits and affects the motion.

$$\mathbf{g}_j^0 = \begin{Bmatrix} g_1^0(\mathbf{r}_i^0, \cdots, \mathbf{r}_n^0) \\ \vdots \\ g_m^0(\mathbf{r}_i^0, \cdots, \mathbf{r}_n^0) \end{Bmatrix} = \mathbf{0} \tag{12}$$

The basic physical equations of Newton and Euler for translational and rotational motion determine the system we need to solve while complying with the constraint equations $\mathbf{g}_j^0 = \mathbf{0} \forall j$:

$$\mathbf{f}_i = m_i * \dot{\mathbf{v}}_i \tag{13}$$

$$\dot{\mathbf{L}}_i = \frac{d(\Theta_i * \omega_i)}{dt} \tag{14}$$

5. Fabrication result

The previous section provided a geometrical understanding of how the hinge parameters change the single unit's deformation. It provided grounding for the hinge foldability and the single DoF of the KinetiX system. To further explore the potential of these parameters in designing deformable structures, we demonstrate a set of tessellated modules with those units while keeping the single DoF with 3D printing. This exploration allows us to design larger scale and compelling transformations arising from single modules. As mentioned in the previous section, some of the configurations are theoretically impossible while physically possible to transform, due to the material and design tolerance. Based on our tolerance test, we found this to not be an barrier for us in fabricating the deformable structures. Therefore, we can focus on showing that our parametric methods are able to achieve a multitude of transformations.

All models are printed with the Stratasys Connex500. The bar is printed with rigid polymer (Vero Series) and the hinge is replaced by elastic polymer (Tango Series) or a rotary rigid hinge (Vero Series).

5.1. Single unit

Five single units (Fig. 12) of planar and spatial transformation are printed with rigid rotary hinges. The printed physical transformation matches with our geometrical prediction and simulation. As Fig. 12.E shows, the physical model of in-plane rotation hinge units can be deformed physically while impossible theoretically. This is due to the gap between the axis rod and the tube of the printed hinge. To further test the deformability in relation to the hinge tolerance, we printed five twisting samples with variable hinge tolerance. Each test unit is printed with VeroBlack Series material. The size of the unit is 3 by 3 cm. The wall thickness is 2 mm. The hinge tolerances are 0.05, 0.1, 0.15, 0.2 and 0.25 mm, respectively. We found that even at the tightest situation (0.05 mm, limited by the printer resolution), the hinge in-plane rotation can still
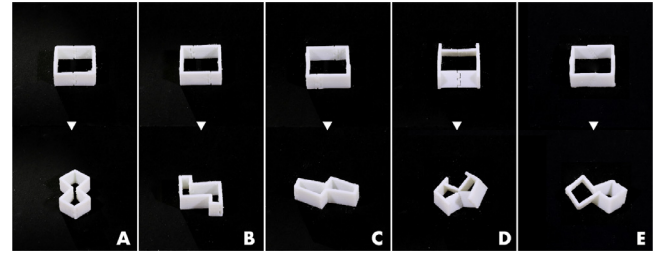

Fig. 12. Five fabricated unit of planar and spatial transformation. (A). the basic unit; (B). planar transformation of uniform scaling; (C). planar transformation of shearing; (D). spatial transformation of bending; (E). spatial transformation of twisting.

Fig. 13. A 15 by 15 identical unit KinetiX panel can be fabricated by simple propagation. The piece exhibits the known auxetic effect. (A). Printed piece; (B). After compression; (C). The hinge configuration.

Fig. 14. An 8 by 8 gradient unit KinetiX panel. The hinges gradually shift their position from left to right. (A). Printed piece; (B). After compression; (C). The hinge configuration.

generate a twist transformation unit. The smaller the tolerance is, the higher the resistance of rotation becomes. As our paper focuses on the study of transformation, we believe the mechanical property of hinges would be interesting to be further investigated in the future.

5.2. Single unit tessellation

A single transformation unit can be combined with identical ones to form larger scaling or shearing transformations, while maintaining a limited DoF as $M = 1$. This is possible with the two types of planar transformation units, uniform scaling, and shearing. When one hinge is deformed, the whole system will transform accordingly. Fig. 13 demonstrates a large printed KinetiX panel with a single unit tessellation. As we mentioned in Section 3.2, shifting the position of the hinge on the wall plane will not affect the foldability and the DoF of the system. We can therefore parametrically tune the position of the hinge to create a gradual change of the transformation. Fig. 14 shows a structure that shears upwards on the left and right side. In this case, the position of the four hinges linearly changes from $P = (0.8, 0.8, 0.8, 0.8)$ to $P = (0.2, 0.2, 0.2, 0.2)$.

In order to construct a line or surface structure with the spatial transformation units, we need to combine them with a planar/spatial transformation unit. The reason is that, in a structure with two units, a deformation in one causes a deformation in the other in an opposite way. This makes the transformation of a single unit a cancelling action, as we described in Section 8. To

Fig. 15. A 1D tessellation of spatial transformation of bending and twisting. This tessellation creates a curling strip.
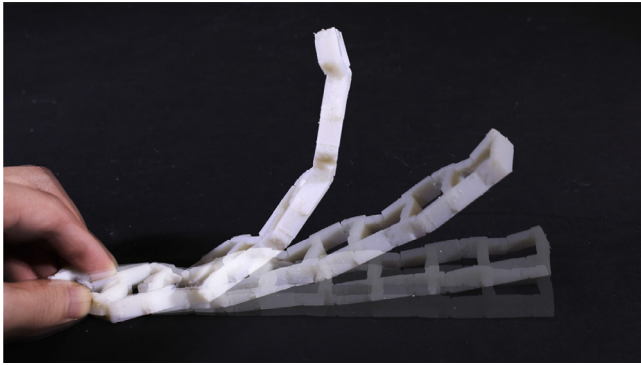
Fig. 16. A 1D tessellation of spatial transformation of bending and basic units. This tessellation creates a bending strip.

resolve this, we can integrate one basic unit between the two in order to convert the transformation. We will further discuss this phenomenon in the following section.

5.3. Multiple Units tessellation

Now that we have facilitated both planar and spatial transformations, we experimented combining two different KinetiX units to create large line and surface tessellations. To guide the experiment, we created a table of possible two units tessellation, where a unit of variable hinge in-plane position, hinge in-plane rotation, or hinge out-of-plane rotation can be combined with other units. (Fig. 20)

This table would enable designers to preliminarily assign two different units into one grid system to get different transformations at desired locations. Based on the two-unit tessellation, one can also choose to have multiple units in order to achieve desired transformation.

To demonstrate the tessellation, we designed and printed four samples that can transform upon compression. They are:

- Hinge out-of-plane rotation + Hinge in-plane rotation to create a curling line; (Fig. 15)
- Hinge out-of-plane rotation + Hinge in-plane position to create a bending line; (Fig. 16)
- Hinge in-plane rotation + Hinge in-plane position to create a twisting line; (Fig. 17)
- Hinge out-of-plane rotation + Hinge in-plane position to create a bending surface; (Fig. 18)
- Hinge out-of-plane rotation + Hinge in-plane position to create a curling surface. (Fig. 19)
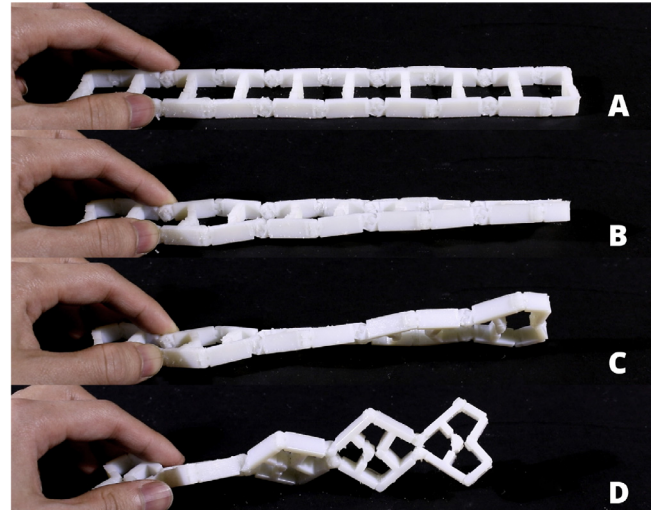
Fig. 17. A 1D tessellation of spatial transformation of twisting and basic units. This tessellation creates a twisting strip.
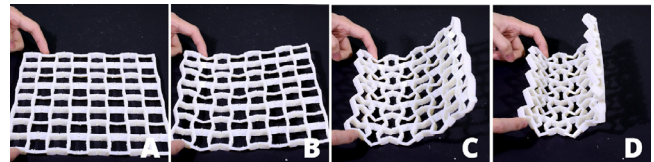
Fig. 18. A 2D tessellation of spatial transformation of bending and basic units. This tessellation creates a bending sheet.
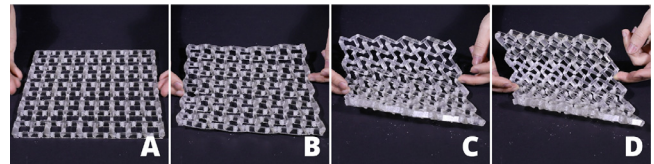
Fig. 19. A 2D tessellation of spatial transformation of bending and planar transformation of shearing. This tessellation creates a curling sheet.
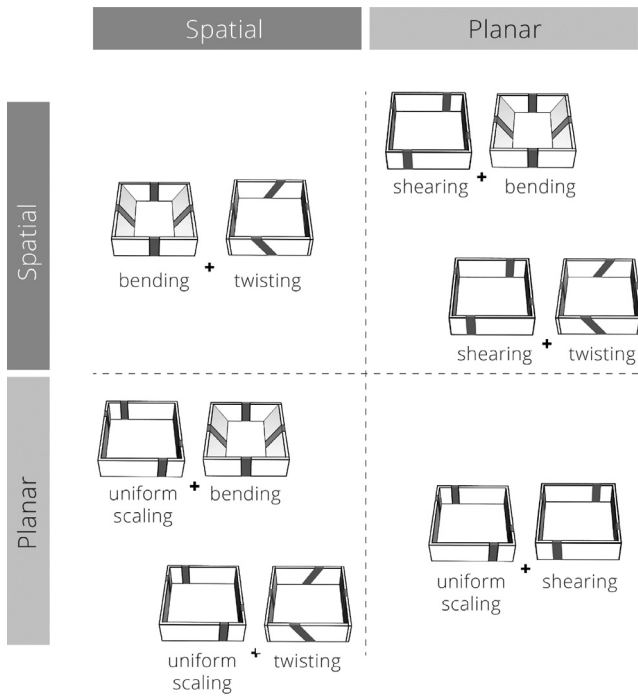
6. Applications

6.1. Encoded display

With the simulation environment we built, we created an application of an encoded display. The display is constructed with a basic unit and the user can partially replace individual units with the uniform scaling unit, to create geometrical shapes or letters. Fig. 21 shows an encoded letter T and Fig. 22 shows an encoded circle shape. Both hinge configurations appear to be identical in the grid before compression. After being compressed, the structures deform differently and reveal the content.

The rigid bars were printed with VeroBlack and the hinges were printed as elastic blocks with TangoBlack, so that the whole grid structure appears identical at each position before compression. The mechanism is still valid if the rotary hinges were used.

6.2. Easy packaging

The rise of the e-commerce in the past decade dramatically increased the need for individual packaging of everything we use in daily life. As KinetiX has a limited single DoF, we imagine this could be applied to a new type of packaging design, one that is self-folding with single direction of force. Fig. 23 shows a cube can be folded when the bottom side is compressed. The cube is

Fig. 20. KinetiX transformable unit composite table. Spatial transformation includes bending and twisting. Planar transformation includes uniform scaling and shearing.
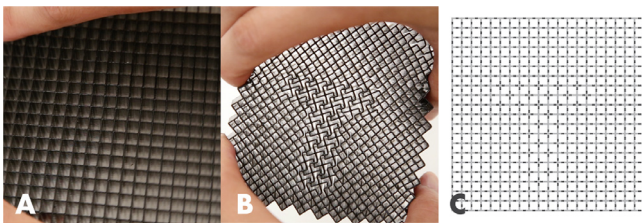
Fig. 21. Application: encoded display. Letter T. (A). before compression; (B). after compression; (C). hinge position.
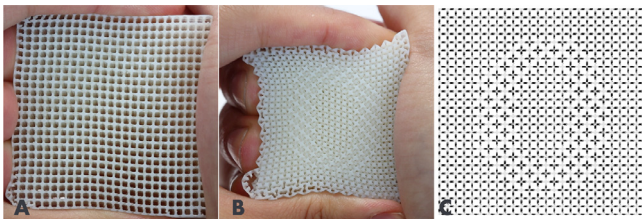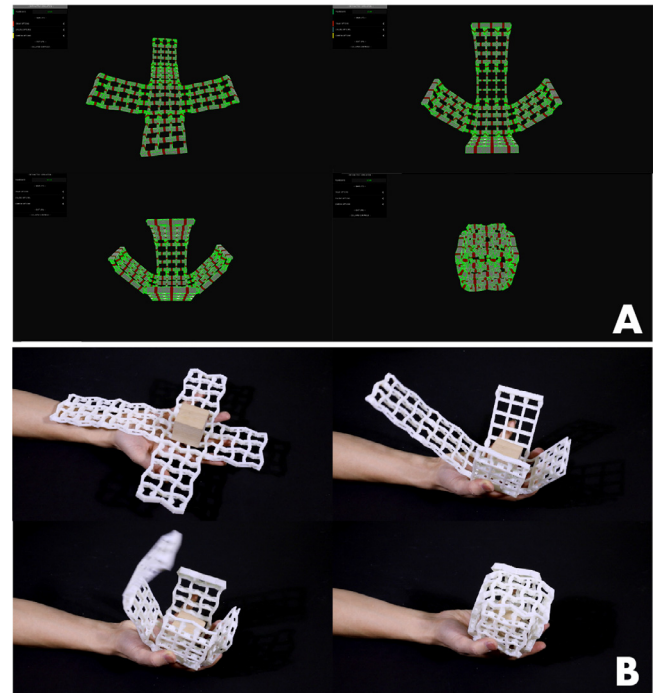

Fig. 22. Application: encoded display. Circle shape. (A). before compression; (B). after compression; (C). hinge position.

Fig. 23. A cubic package prototype can be folded from flat when the bottom side is compressed. (A). A simulation of the package transforming. (B). A fabricated package.

Fig. 24. A prototype of foldable helmet based on the structures of KinetiX. (A). Simulation of the helmet folding; (B). Fabricated helmet.

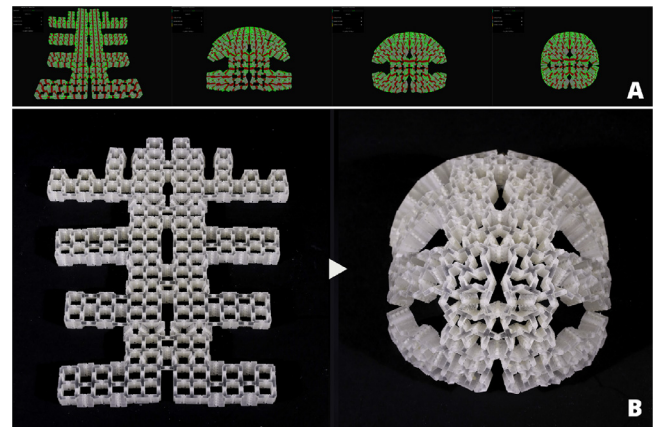**Fig. 25.** The helmet fit on a male styrofoam head.

designed empirically with the help of the simulation tool. We adjusted the degree of out-plane hinge rotation so that it produces an approximate 90 degree folding. The hinges are then used on the five "creases", while the six sides of the cube are constructed with the basic unit.
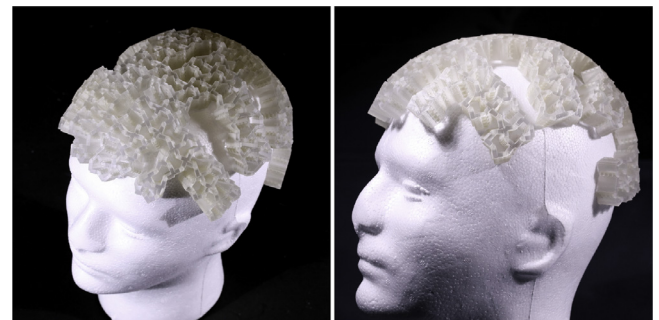
6.3. Conformable helmet

To demonstrate the transformation tunability of KinetiX, we present a prototype of a conformable helmet. The helmet is printed flat to save printing time, and is able to fold to wrap around one's head with a single DoF. We designed this helmet with the following process: (1). Use paper to wrap around the styrofoam mannequin head and cut off the excessive overlapping parts. (2). This gives us a rib-like structure when the paper is laid flat. (3). Empir-

ically apply the KinetiX units, bending and basic ones, to the rib-like structure. (4). Feed the 3D model into the simulation system and see the folding result. (5). Re-iterate the units design based on the simulation result. (6). After 4 iterations, we achieved a helmet that approximately conforms to a life-sized styrofoam head.

7. Limitations and future works

The KinetiX presents a set of novel cell designs that extends the current studies on auxetic materials. While introducing the hinge parameters gives us the ability to design interesting transformations like bending or twisting, we would like also to point out the limitations of work.

- Arbitrary Parameters: As we mentioned in the Section 3.2, arbitrarily assigning the positions to four hinges on the bars could also achieve an $M = 1$ DoF for a unit. However, it also creates non-uniform transformations, which might not be desirable in a design process. In addition, the hinge in-plane and out-plane rotation angles need to be symmetrically mirrored. Arbitrary angles will create an $M = 0$ DoF for the unit, and therefore not useful for the design.
- Hinge Design: While fabricating smaller length scale of the physical unit models is highly desirable, we are also limited by the 3D printer's material properties. During our study, we found that a reliable hinge diameter should be no less than 1 mm for the sake of durability. The hinge tolerance should be higher than 0.03 mm to avoid material fusing in the hinge during the print.
- Beyond Square Unit: So far, we have demonstrated our process on square transformable units. We can also expand this mechanism to other shapes. Since the basic mechanism of KinetiX is a four-bar linkage structure, as long as we keep the hinge configuration, the changes of the bar shape will not affect the unit's DoF. However, this work only focuses on the square unit design as other shapes might introduce complex collisions that affect the transformation.

Towards the future, we believe the following aspects should be improved:

- Mechanism Model: Currently we use our simulation tool to iterate design. An in-depth modelling of KinetiX structures should be conducted to better understand tunability. This would help us to better understand the energy dissipation across the system and therefore suggest suitable strategies for applying deformation forces. We would also like to further explore the transformation space of 3D lattice configurations, beyond 2D panel, of KinetiX.
- Design and Optimization: While our simulation environment allows us to iterate upon designs before physically fabricating them, we would like to develop a design tool for designers to easily create KinetiX structures, and create a goal-oriented design pipeline by including an optimization process. This would dramatically shorten the design process and improve transformation accuracy.
- Fabrication: The mechanism of KinetiX is universal. It is worthy to experiment using other fabrication methods such as injection molding and assembly to create material structures of sizes that exceed the build platform size of a 3D printer and also improve the material quality.
- Actuation: We would like to experiment with actuation method. It has been reported [29,30] that specific 3D printed materials have shape-memory effects. With the KinetiX mechanism, we can create self-actuated structures under temperature change.

8. Conclusion

In this paper we introduced a mechanism of creating deformable materials that is inspired by a type of auxetic structure. The structure we developed is a cellular-based material design composed of rigid plates and elastic hinges. Different compositions of these elements lead to a multitude of shape-changing possibilities and create materials that exhibit mechanical transformations such as uniform scaling, shearing, bending and rotating. We presented a numerical analysis of the structure and a simulation environment to preview the transformation. We also provided examples of how such structures can be applied in product design and next generation packaging. As the resolution and quality of 3D printing improves, the proposed structures may be miniaturized. We believe the proposed cell designs enable the design of a new class of deformable material across length and scales.

References

[1] Yao L, Niiyama R, Ou J, Follmer S, Della Silva C, Ishii H. Pneui: pneumatically actuated soft composite materials for shape changing interfaces. In: Proceedings of the 26th annual ACM symposium on user interface software and technology UIST '13. New York, NY, USA: ACM; 2013. p. 13–22. ISBN 978-1-4503-2268-3. http://doi.acm.org/10.1145/2501988.2502037.

[2] Panetta J, Zhou Q, Malomo L, Pietroni N, Cignoni P, Zorin D. Elastic textures for additive fabrication. ACM Trans Graph 2015;34(4):135:1–135:12. http://doi.acm.org/10.1145/2766937.

[3] Bickel B, Bächer M, Otaduy MA, Lee HR, Pfister H, Gross M, et al. Design and fabrication of materials with desired deformation behavior. ACM Trans Graph (Proc SIGGRAPH) 2010;29(3).

[4] Ou J, Yao L, Tauber D, Steimle J, Niiyama R, Ishii H. jamsheets: Thin interfaces with tunable stiffness enabled by layer jamming. In: Proceedings of the eighth international conference on tangible, embedded and embodied interaction, TEI '14. New York, NY, USA: ACM; 2013. p. 65–72. ISBN978-1-4503-2635-3. http://doi.acm.org/10.1145/2540930.2540971.

[5] Ou J, Skouras M, Vlavianos N, Heibeck F, Cheng CY, Peters J, et al. Aeromorph - heat-sealing inflatable shape-change materials for interaction design. In: Proceedings of the 29th annual symposium on user interface software and technology, UIST '16. New York, NY, USA: ACM; 2016. p. 121–32. ISBN978-1-4503-4189-9 http://doi.acm.org/10.1145/2984511.2984520.

[6] Ion A, Frohnhofen J, Wall L, Kovacs R, Alistar M, Lindsay J, et al. Metamaterial mechanisms. In: Proceedings of the 29th annual symposium on user interface software and technology, UIST '16. New York, NY, USA: ACM; 2016. p. 529–39. ISBN978-1-4503-4189-9 http://doi.acm.org/10.1145/2984511.2984540.

[7] Iwafune M, Ohshima T, Ochiai Y. Coded skeleton: programmable bodies for shape changing user interfaces. In: Proceedings of the ACM SIGGRAPH 2016 PostersSIGGRAPH '16. New York, NY, USA: ACM; 2016. p. 18:1–18:2. ISBN 978-1-4503-4371-8. http://doi.acm.org/10.1145/2945078.2945096.

[8] Yao L, Ou J, Cheng CY, Steiner H, Wang W, Wang G, et al. Biologic: natto cells as nanoactuators for shape changing interfaces. In: Proceedings of the 33rd annual ACM conference on human factors in computing systems, CHI '15. New York, NY, USA: ACM; 2015. p. 1–10. ISBN978-1-4503-3145-6. http://doi.acm.org/10.1145/2702123.2702611.

[9] Yasu K, Inami M. Popapy: instant paper craft made up in a microwave oven. In: Proceedings of the ninth international conference on advances in computer entertainment ACE'12. Berlin, Heidelberg: Springer-Verlag; 2012. p. 406–20. ISBN 978-3-642-34291-2. https://doi.org/10.1007/978-3-642-34292-9_29.

[10] Raviv D, Zhao W, McKnelly C, Papadopoulou A, Kadambi A, Shi B, et al. Active printed materials for complex self-evolving deformations. Sci Rep 2014;4:7422EP. https://doi.org/10.1038/srep07422; article.

[11] Mir M, Najabat AM, Sami J, Ansari U. Review of mechanics and applications of auxetic structures. Adv Mater Sci Eng 2014. Article.

[12] Saxena KK, Das R, Calius EP. Three decades of auxetics researchaterials with negative Poisson's ratio: a review. Adv Eng Mater 2016;18(11):1847–70. https://doi.org/10.1002/adem.201600053.

[13] Bertoldi K, Vitelli V, Christensen J, van Hecke M. Flexible mechanical metamaterials. Nat Rev 2017;2:17066.

[14] Kolken HA, Zadpoor AA. Auxetic mechanical metamaterials. RSC Adv 2017;7:5111–29. https://doi.org/10.1039/C6RA27333E.

[15] Choi JB, Lakes RS. Non-linear properties of metallic cellular materials with a negative Poisson's ratio. J Mater Sci 1992;27(19):5375–81. https://doi.org/10.1007/BF00553421.

[16] Lakes R, Elms K. Indentability of conventional and negative Poisson's ratio foams. J Compos Mater 1993;27(12):1193–202. 10.1177/002199839302701203. doi:10.1177/002199839302701203.

[17] Choi JB, Lakes RS. Fracture toughness of re-entrant foam materials with a negative Poisson's ratio: experiment and analysis. Int J Fract 1996;80(1):73–83. https://doi.org/10.1007/BF00036481.

[18] Chen CP, Lakes RS. Micromechanical analysis of dynamic behavior of conventional and negative Poissons ratio foams. J Eng Mater Technol 1996;118(3):285–8. https://doi.org/10.1115/1.2806807.

[19] Wang P, Casadei F, Shan S, Weaver JC, Bertoldi K. Harnessing buckling to design tunable locally resonant acoustic metamaterials. Phys Rev Lett 2014;113:014301.

[20] Hoberman C. Hoberman sphere. 1990. http://www.hoberman.com/.

[21] Fischer U., Heine K.A. Tabula Rasa' table. 1987. http://catalog.quittenbaum.de.

[22] Overvelde JTB, Weaver JC, Hoberman C, Bertoldi K. Rational design of reconfigurable prismatic architected materials. Nature 2017;541:347–52.

[23] Coelho M, Maes P. Shutters: a permeable surface for environmental control and communication. In: Proceedings of the third international conference on tangible and embedded interaction, TEI '09. New York, NY, USA: ACM; 2009. p. 13–18. ISBN 978-1-60558-493-5. http://doi.acm.org/10.1145/1517664.1517671.

[24] Bau O, Petrevski U, Mackay W. Bubblewrap: a textile-based electromagnetic haptic display. In: Proceedings of the CHI '09 extended abstracts on human factors in computing systems, CHI EA '09. New York, NY, USA: ACM; 2009. p. 3607–12. ISBN 978-1-60558-247-4 http://doi.acm.org/10.1145/1520340.1520542.

[25] Skouras M, Thomaszewski B, Coros S, Bickel B, Gross M. Computational design of actuated deformable characters. ACM Trans Graph 2013;32(4):82:1–82:10. http://doi.acm.org/10.1145/2461912.2461979.

[26] Grima JN, Manicaro E, Attard D. Auxetic behaviour from connected different-sized squares and rectangles. Proc Royal Soc Lond A: Math Phys Eng Sci 2010.

[27] Coumans E. Bullet physics simulation. In: Proceedings of the ACM SIGGRAPH 2015 Courses, SIGGRAPH '15. New York, NY, USA: ACM; 2015. ISBN 978-1-4503-3634-5. http://doi.acm.org/10.1145/2776880.2792704.

[28] Mamou K. Github repository of v-hacd. https://github.com/kmammou/v-hacd; 2017.

[29] Mao Y, Ding Z, Yuan C, Ai S, Isakov M, Wu J, et al. 3d printed reversible shape changing components with stimuli responsive materials. Sci Rep 2016;6. https://doi.org/10.1038/srep24761.

[30] Liu K, Wu J, Paulino GH, Qi HJ. rogrammable deployment of tensegrity structures by stimulus-responsive polymers. Sci Rep 2017;7(1):3511. https://doi.org/10.1038/s41598-017-03412-6.